ACCSCIENCE PUBLISHING

Tumor Discovery

ORIGINAL RESEARCH ARTICLE

Profiling energy metabolism in normal bladder tissue and non-muscle-invasive bladder cancer cases of different histological grades

Guilherme Prado Costa[1,2], Petra Karla Böckelmann[1], Renato Prado Costa[2], Carlos Hermann Schaal[2], Fernando César Sala[2], André Pereira Vanni[2], Leandro Luiz Lopes de Freitas[3], João Carlos Cardoso Alonso[1,4], Gabriela Cardoso de Arruda Camargo[1], Gabriela de Oliveira[1], Bianca Ribeiro de Souza[5], Athanase Billis[3], and Wagner José Fávaro[1]*

[1]Laboratory of Urogenital Carcinogenesis and Immunotherapy (LCURGIN), Universidade Estadual de Campinas (UNICAMP), Campinas City, São Paulo State, Brazil

[2]Department of Urology, Amaral Carvalho Hospital (HAC), Jaú City, São Paulo State, Brazil

[3]Department of Pathology, Medical School, Universidade Estadual de Campinas (UNICAMP), Campinas City, São Paulo State, Brazil

[4]Department of Urology, Paulínia Municipal Hospital, Paulínia City, São Paulo State, Brazil

[5]Department of Obstetrics and Gynecology, OVCARE, University of British Columbia, Vancouver, British Columbia, Canada

Abstract

Bladder cancer (BC) stands as the second most common urinary tract malignancy. Recent years have witnessed a growing interest in investigating energy metabolism to help with better understanding the energy sources harnessed by tumor cells. The aims of the present study are to feature and compare cell energy metabolism profiles among different histological grades of non-muscle-invasive BC (NMIBC) by adjusting their bioenergetic cellular indexes based on the specific tumor types. Forty urinary bladder tissue samples from patients both with and without a diagnosis of urothelial lesions were collected. Subsequently, samples were categorized into four groups comprising ten samples each, namely: normal (no urothelial lesions) group, low-grade pTa group, high-grade pTa group, and high-grade pT1 group. These tissue samples were examined by means of immunohistochemistry and Western blotting to assess proteins involved in cell energy metabolism. Based on the current findings, the normal and low-grade pTa groups presented clear preference for the oxidative phosphorylation pathway; consequently, they recorded high bioenergetic cellular index. On the other hand, both the high-grade pTa and pT1 groups presented proclivity towards the glycolytic pathway. These observations, mainly those associated with the bioenergetic cellular index, hold promising clinical relevance in the management of BC. Given the often aggressive and potentially debilitating nature of treatments applied to this neoplasia type, the current study offers invaluable insights on this topic and emphasizes changes in the bioenergetic cellular index at different NMIBC grades, which could serve as potential markers for both the diagnosis and prognosis of NMIBC patients.

Keywords: Bladder cancer; Energy metabolism; Bioenergetic cellular index; Cancer metabolism

***Corresponding author:**
Wagner José Fávaro
(favarowj@unicamp.br)

Citation: Costa GP, Böckelmann PK, Costa RP, *et al*. Profiling energy metabolism in normal bladder tissue and non-muscle-invasive bladder cancer cases of different histological grades. *Tumor Discov*. 2024:3(1):2290. https://doi.org/10.36922/td.2290

Received: November 22, 2023
Accepted: January 9, 2024
Published Online: March 19, 2024

Copyright: © 2024 Author(s). This is an Open-Access article distributed under the terms of the Creative Commons Attribution License, permitting distribution, and reproduction in any medium, provided the original work is properly cited.

Publisher's Note: AccScience Publishing remains neutral with regard to jurisdictional claims in published maps and institutional affiliations.

1. Introduction

Bladder cancer (BC) emerges as a significant global public health concern due to the elevated morbidity and mortality rates.[1] Notably, BC tends to be recurrent and aggressive in terms of progression, even in cases at localized disease stages.[1,2] Patients diagnosed with BC often require multiple intravesical treatments, while advanced and metastatic cases are treated with intricate surgical and systemic interventions. Consequently, BC imposes a substantial burden on health-care resources, resulting in significant economic costs.[1,3]

Non-muscle-invasive BC (NMIBC) accounts for the majority of bladder tumor cases, comprising 70 – 75% of the cases. NMIBC is characterized by the confinement of tumor to the urothelium as papillary tumor (pTa) or carcinoma *in situ* (pTis or CIS) without stromal invasion or with limited invasion into the lamina propria (pT1).[4,5] This cancer type encompasses a diverse group of tumors, with progression rates to the muscle-invasive phenotype ranging from 0.8% to 50% within 5 years,[6,7] as indicated by previous studies. Notably, significant risk factors for NMIBC progression include the concurrent presence of CIS, high tumor grade, and T1 stage.[6,7] In addition, factors such as multiplicity, tumor size ≥3 cm, and a history of relapse are also considered risk factors for this disease.[6,7]

Low-grade Ta tumors present relapse rates up to 50%, and they only progress in 5% of cases. Conversely, high-grade T1 tumors show relapse rates exceeding 80%, and over 50% of cases progress within the initial 3 years.[8,9] Chromosomal changes stemming from DNA strand oxidation. Chromosomal changes resulting from DNA strand oxidation affect the functions of oncogenes and tumor suppressor genes, as well as trigger different biological behaviors in low- and high-grade BC. Notably, low-grade BC tends to manifest as superficial, papillary, and indolent tumors, whereas high-grade BC are prone to relapse and to progress into invasive muscle tissue.[8] Moreover, other prognostic factors, such as tumor size, multifocality, papillary versus sessile appearance, and lymphovascular invasion hold clinical significance.[10] These behavioral variations may be intricately linked to cell energy metabolism profiles presented by different histological grades of NMIBC. Analyzing and understanding metabolic adaptation strategies adopted by neoplastic cells to meet the high cell growth and proliferation demands within each histological grade of NMIBC is a promising approach to acquiring more comprehensive knowledge on their behavior.

Cancer onset and advancement are intricately linked to changes in cell metabolism, which provide energy to support cell growth and fast proliferation.[11] These metabolic adaptations encompass increased oxygen consumption, nutrient depletion, as well as the generation of reactive nitrogen and oxygen intermediates. The Warburg effect is a prominent metabolic phenomenon observed in cancer cells.[11,12] This effect involves preference for aerobic glycolysis and lactate fermentation over oxidative phosphorylation, even in the presence of abundant oxygen and fully functional mitochondria. This metabolic shift serves the essential purpose of meeting the increased energy demands necessary for the synthesis of lipids, proteins, and nucleic acids of the cancer cells. Thus, Warburg effect stands out as a pivotal feature of BC cancer cells, as well as of different solid tumor types.[11]

Metabolic activity in normal cells primarily relies on oxidative phosphorylation, which is a highly efficient process that generates abundant adenosine triphosphate (ATP) in comparison to glycolysis. Glucose is converted into pyruvate through glycolysis within the cytosol in physiologically normal cells, and subsequently, it is turned into carbon dioxide in the mitochondria, mainly under aerobic conditions.[11,13] However, glycolysis takes precedence under anaerobic conditions, and it results in limited pyruvate supply to the oxygen-consuming mitochondria.[11,13] This metabolic shift is featured by high glucose consumption and by lactate production, regardless of oxygen availability.[11,13-16]

Several key proteins participating in both the oxidative phosphorylation and glycolysis pathways can be utilized as markers to assess the activity of these metabolic processes. Glucose transporter-1 (GLUT1), phosphofructokinase (PFK), glyceraldehyde 3-phosphate dehydrogenase (GAPDH), and lactate dehydrogenase A (LDH-A) are used as glycolytic pathway markers. Moreover, pyruvate dehydrogenase (PDH), citrate synthase (CS), short chain 3-hydroxyacyl-CoA dehydrogenase (HADHSC), mitochondrial ATP synthase F1-beta-subunit (β-F1-ATP synthase), and heat shock protein 60 (hsp60) are used as oxidative phosphorylation pathway markers.

Several previous studies have focused on investigating the mitochondrial energy metabolism of neoplastic cells and assessed the β-catalytic subunit concentration within the H+-ATP synthase complex as oxidative phosphorylation marker. These studies have also investigated hsp60 as marker of mitochondrial structural proteins, in association with GAPDH, which was used as glycolytic pathway marker. These data make it feasible to calculate the bioenergetic cellular index (IBEC) through the following equation:[17-19]

$$\mathrm{IBEC} = \frac{\beta - \mathrm{F1} - \mathrm{ATPase}}{\mathrm{hsp60\,x\,GAPDH}} \quad (1)$$

In light of the foregoing, the aims of the current study were to feature and compare the cell energy metabolism profiles among normal bladder tissue and NMIBC tissues with different histological grades (low-grade pTa, high-grade pTa, and high-grade pT1). The present research adjusted the IBEC to these specific tumor types in order to establish a clinically relevant criterion with prognostic significance to classify this neoplasia.

2. Materials and methods

2.1. Human samples

This retrospective study analyzed 40 urinary bladder tissue samples from patients (median age of 62 years) both with and without a diagnosis of urothelial lesions by maintaining male-to-female ratio of 2:1. Tissue specimens were obtained at the Urology Service at Amaral Carvalho Hospital, Jaú City, Brazil. Ten bladder tissue samples were sourced from autopsies of patients without a diagnosis of urothelial injury or urological disease. In addition, the remaining 30 bladder tissue samples were obtained from patients who underwent transurethral resection of the bladder tumor (TURBT).

Histopathological diagnoses were meticulously assessed by a senior uropathologist in accordance with the classification consensus put forth by the International Society of Urological Pathology/World Health Organization.[20] The categorization process lied in splitting the samples into three different groups, with each comprising ten samples, namely normal (no urothelial lesions) group, low-grade pTa group, high-grade pTa group, and high-grade pT1 group. Subsequently, these tissue samples were subjected to rigorous analyses using techniques encompassing immunohistochemistry and Western blotting.

All procedures herein were conducted in full compliance with the ethical standards set forth by the Ethics and Research Committee of Amaral Carvalho Hospital, Jaú City, Brazil (CAAE number: 47475815.9.0000.5434).

2.2. Immunohistochemical analysis

The same set of bladder samples (n = 10 per group), which had been previously used for histopathological analysis, was also used for immunolabeling procedures. These tissue samples were cut into 5 μm-thick sections. Antigen retrieval was achieved by subjecting the aforementioned sections to three 5-min heating cycles in 10 mM citrate buffer at pH 6.0, in standard microwave oven. Subsequently, sections were incubated in peroxidase blocker (EasyPath EP12-20523, Sao Paulo, Brazil) and this procedure was followed by incubation in 5% goat serum blocking solution (EasyPath EP12-20523, Sao Paulo, Brazil) at room temperature for 10 min.

Specific antigens corresponding to (GLUT1; rabbit polyclonal antibody, sc7903, Santa Cruz Biotechnology, USA), (PFK; mouse monoclonal antibody, LS-C173559, LifeSpan BioSciences, Inc., USA), (GAPDH; rabbit polyclonal antibody, ab37168, abcam, USA), (LDH; mouse monoclonal antibody, sc137243, Santa Cruz Biotechnology, USA), (PDH; rabbit polyclonal antibody, GTX104040, GeneTex, USA), (CS; mouse monoclonal antibody, sc390693, Santa Cruz Biotechnology, USA), (HADHSC; rabbit polyclonal antibody, sc 292196, Santa Cruz Biotechnology, USA), mitochondrial ATP synthase F1-beta-subunit (β-F1-ATP synthase [ATPase]; rabbit polyclonal antibody, sc134962, Santa Cruz Biotechnology, USA), and (hsp60; mouse monoclonal antibody, sc376240, Santa Cruz Biotechnology, USA) were identified by reacting the tissue specimens with specific primary antibodies, which were diluted in 1% bovine serum albumin (BSA) and stored overnight at 4°C. Bound antibodies were detected based on using EasyLink One kit (EasyPath EP-12-20504, Sao Paulo, Brazil). Subsequently, sections were slightly counterstained with Harris' hematoxylin and visualized in Leica DM2500 microscope equipped with DFC295 camera (Leica, Munich, Germany).[21]

The rate of positively stained cells was assessed in ten fields for each antibody, under high magnification (×400), to assess antigen immunoreactivity intensity within urothelial cells in ImageJ software (https://imagej.nih.gov/ij/). Quantitative data were analyzed in two different manners, namely total immunoreactivity and immunoreactivity intensity. Total immunoreactivity was calculated as complement of the negative rate of urothelial cells observed for a given antibody, subtracted from 100%. In other words, it represented the total number of urothelial cells in the field that presented immunoreactivity to the assessed antibody. Immunoreactivity intensity was assessed based on categorizing the observed immunoreactivity within urothelial cells by taking into consideration intensity criteria. These categories were established in ImageJ software, at scale ranging from 0 to 3 wherein: 0 (no immunoreactivity) means 0% positive urothelial cells, 1 (weak immunoreactivity) indicates 1 – 35% positive urothelial cells, 2 (moderate immunoreactivity) represents 36 – 70% urothelial cells, and 3 (intense immunoreactivity) features >70% positive urothelial cells.[22]

2.3. Western blotting

Urinary bladder samples were collected from all 40 patients and subjected to immunoblotting analysis performed according to the established protocols.[21] In total, 70 μg protein was loaded into each well on the SDS-polyacrylamide gel for electrophoresis. Subsequently, proteins were transferred to nitrocellulose membranes,

which, in turn, were blocked with 3% BSA solution diluted in TBS-T buffer to mitigate non-specific protein binding. Nitrocellulose membranes were incubated overnight with primary antibodies (diluted 1:1000 in 1% BSA), such as GLUT1, PFK, GAPDH, LDH, PDH, CS, HADHSC, β-F1-ATP synthase (ATPase), and hsp60, at 4°C. On completing the primary antibody incubation, membranes were further incubated with secondary HRP-conjugated antibodies (diluted 1:3000 ratio in 1% BSA; MilliporeSigma, USA) for 2 h. Immunoreactive bands were visualized through incubation with 3,3'-diaminobenzidine chromogen (Sigma Chemical Co., St Louis, USA). Immunoblots were run in duplicate, and the samples were grouped into sets comprising 10 samples per group, for each repetition.

Semi-quantitative densitometry analysis was applied to the bands in NIH ImageJ 1.47v software (National Institute of Health, USA, available at: http://rsb.info.nih.gov/ij/), and it was followed by statistical analyses. Results are expressed as mean ± standard deviation of band intensities in comparison to β-actin (which was used as endogenous positive control) labeling intensity.[21]

2.4. IBEC

The IBEC was calculated from several parameters determined based on the established protocols using Equation 1.[17,18,23]

2.5. Statistical analysis

Quantitative results are expressed as mean ± standard deviation, whenever appropriate. Comparison of immunohistochemical and Western blotting data among the investigated groups were analyzed using one-way analysis of variance, followed by Tukey test, at 1% significance level (P <0.01). IBEC assessment was performed using Student's t-test for paired samples.

3. Results

3.1. Patients' baseline demographic and general features

The study included 40 patients who were divided into four groups, with each comprising 10 patients. The median age of the patients was 62.5 years, and the male-to-female ratio was 2:1. With respect to BC risk factors, 70.0% (28/40) of patients were smokers. Prior TURBT was observed in 12.5% (5/40) of patients, whereas Bacillus Calmette–Guérin (BCG) therapy had been administered in only 2.5% of cases. This study only included cases whose specimens were of the same tumor stage and grade as the corresponding specimens assessed during the prior TURBT. The median size observed for low-grade pTa tumors was 3.0 cm, whereas that observed for high-grade pTa tumors was 3.0 cm, and the one for high-grade pT1 tumors was 4.0 cm (Table 1).

Each sample collected from urinary bladders was classified based on their histopathological grade. After the classification procedure, the samples were divided into four groups based on histopathological grade, namely, normal (no urothelial lesions) group, low-grade pTa group, high-grade pTa group, and high-grade pT1 group. Samples belonging to the low-grade pTa group showed extensive papillary lesions. Urothelial cells presented overall orderly appearance with minimal variability in their architecture and cytological features, lack of nuclear hyperchromasia, and infrequent miotic figures (Figure 1A and B). High-grade pTa group samples also presented extensive papillary lesions but featured disorderly arranged urothelial cells, significant cell pleomorphism, nuclear hyperchromasia, and several mitotic figures (Figure 1C and D). On the other hand, the high-grade pT1 group samples presented basement membrane rupture with consequent invasion of neoplastic urothelial cells arranged in cords or nests on the lamina propria. Neoplastic urothelial cells presented eosinophilic cytoplasm and a large number of hyperchromatic nuclei and mitotic figures (Figure 1E and F).

3.2. The oxidative phosphorylation pathway prevailed in normal bladder tissue and low-grade pTa bladder tumor

Intense immunoreactivity was observed for β-F1-ATP synthase (ATPase), HADHSC, PDH, and CS, within the

Table 1. Baseline characteristics

	No lesions	Non-muscle-invasive bladder cancer		
	Normal	Low-grade pTa	High-grade pTa	High-grade pT1
Patients (n)	10	10	10	10
Male/Female	7/3	8/2	7/3	8/2
Age (years in median)	61	56	62	71
Smoking (yes/no)	3/7	8/2	8/2	9/1
Previous TURBT (yes/no)	0/10	1/9	2/8	2/8
Previous BCG (yes/no)	0/10	0/10	0/10	1/9
Lesion size (median)	0	3.0 cm	3.0 cm	4.0 cm

Abbreviations: BCG: Bacillus Calmette–Guérin; TURBT: Transurethral resection of the bladder tumor.

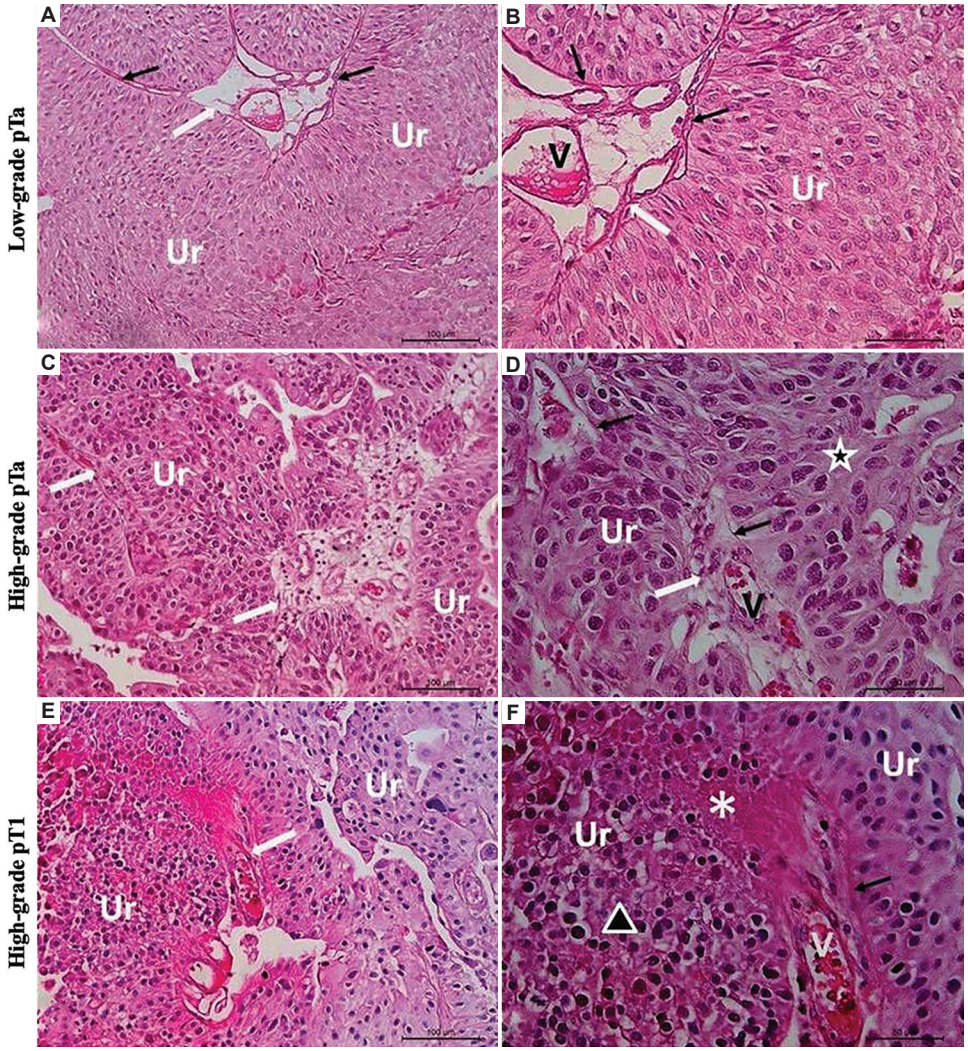


Figure 1. Urinary bladder photomicrographs of low-grade pTa group (A and B), high-grade pTa group (C and D), and high-grade pT1 group (E and F). (A and B) Urothelial cells presenting overall orderly appearance with minimal variability in architecture and cytological features, no nuclear hyperchromasia, and infrequent mitotic figures. (C and D) Significant cell pleomorphism, notable cell atypia (star), and several mitotic figures. (E and F) Basement membrane disruption (asterisk) with neoplastic cells' invasion in the lamina propria. Abbreviations and symbols: Ur: Urothelium; V: Blood vessel; white arrow, conjunctive-vascular axis; black arrow, basal membrane integrity; star, cell atypia; asterisk, basement membrane disruption. Scale bars: 100 µm (panels A, C, and E), and 50 µm (panels B, D, and F).

cohort of normal bladder tissue samples and low-grade pTa tumors, as shown in Figures 2A-D, 3A, 3D, 3G, and 3J, respectively. On the other hand, the high-grade pTa group recorded moderate immunoreactivity level for these proteins, as shown in Figure 3B, E, H, and K, whereas the pT1 group recorded weaker immunoreactivity patterns for the same set of proteins, as evidenced in Figure 3C, F, I, and L. The mean immunolabelled antigen intensities in urinary bladder samples from the normal, low-grade pTa, high-grade pTa, and high-grade pT1 groups are tabulated in Table 2.

The normal and low-grade pTa groups recorded protein levels significantly higher than those of the high-grade pTa and pT1 groups for β-F1-ATP synthase, HADHSC, and PDH, as indicated in Figure 4A-C, respectively. Interestingly, CS protein levels were significantly higher in normal group when compared to other groups (Figure 4D). Furthermore, no statistically significant differences in CS protein levels were observed among the low-grade pTa, high-grade pTa, and high-grade pT1 groups, as shown in Figure 3D.

3.3. The glycolytic pathway prevailed in high-grade pTa and high-grade pT1 bladder tumors

Intense immunoreactivity levels were observed for GLUT1 and PFK in the high-grade pTa and high-

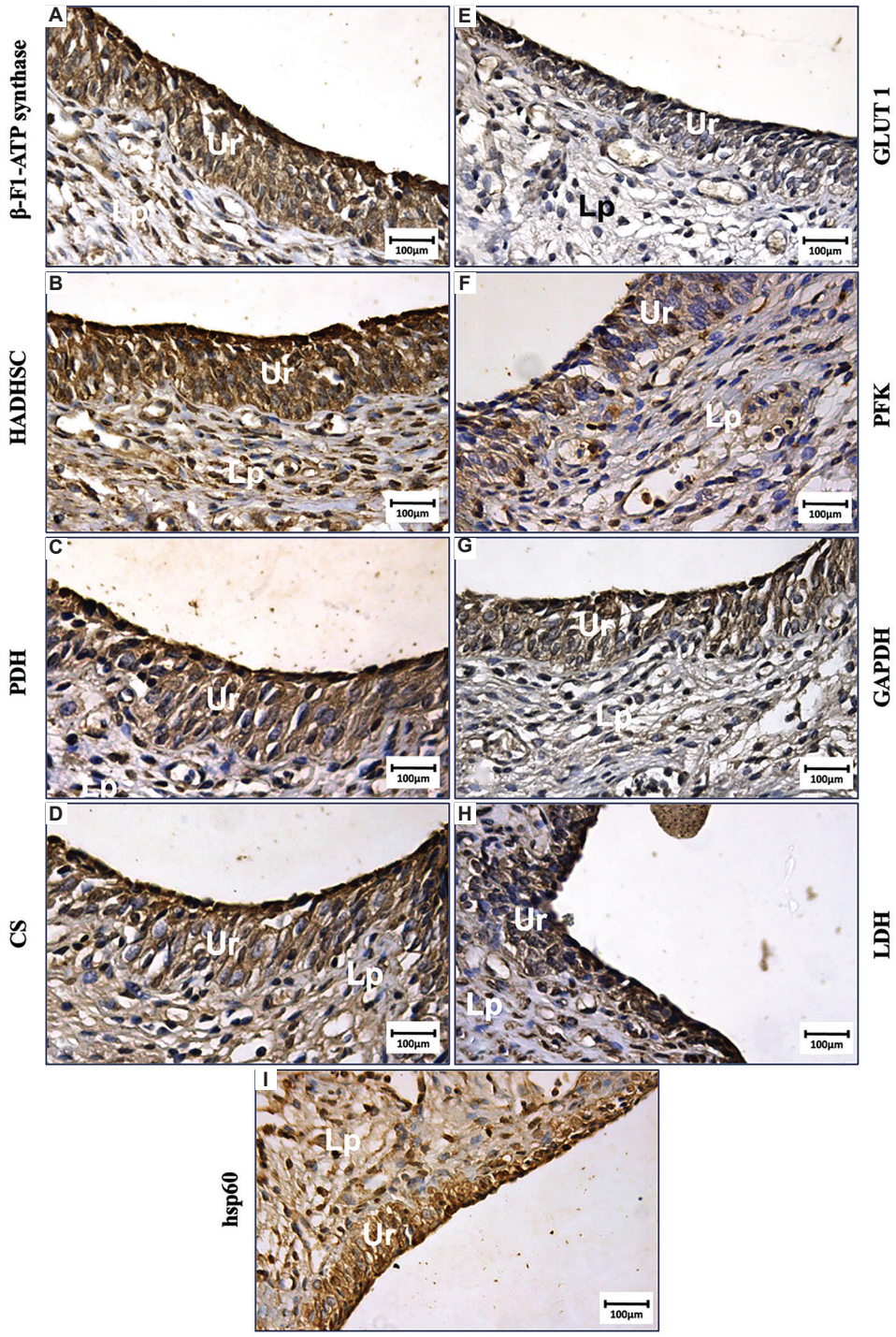


Figure 2. Immunohistochemical results of urinary bladder in normal bladder tissue group: β-F1-ATP synthase (A), HADHSC (B), PDH (C), CS (D), GLUT1 (E), PFK (F), GAPDH (G), LDH (H), and hsp60 (I). Scale bar: 100 μm.
Abbreviations: Lp: Lamina propria; Ur: Urothelium, ATP: Adenosine triphosphate; GLUT1: Glucose transporter-1; PFK: Phosphofructokinase; GAPDH: Glyceraldehyde 3-phosphate dehydrogenase; LDH: Lactate dehydrogenase; PDH: Pyruvate dehydrogenase; CS: Citrate synthase; HADHSC: Short chain 3-hydroxyacyl-CoA dehydrogenase; hsp60: Heat shock protein 60.

grade pT1 groups, as shown in Figure 5B, C, E, and F, unlike the weak immunoreactivity levels observed in the normal (Figure 2E and F) and low-grade pTa groups (Figure 5A and D), respectively (Table 2).

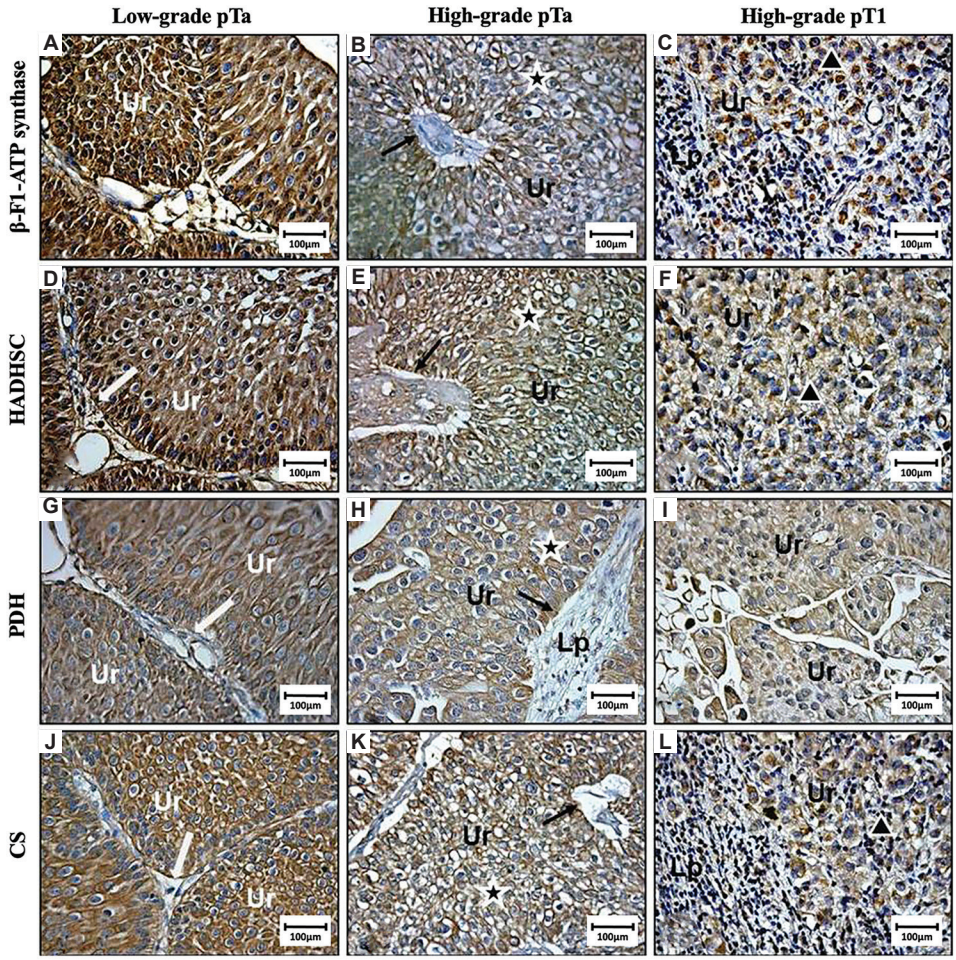


Figure 3. Immunohistochemical results of urinary bladder in low-grade pTa group (A, D, G, and J), high-grade pTa group (B, E, H, and K), and high-grade pT1 group (C, F, I, and L). Cytoplasmic immunoreactivity was observed for β-F1-ATP synthase (A, B, and C), HADHSC (D, E, and F), PDH (G, H, and I), and CS (J, K, and L) protein levels in urothelial cells. Scale bar: 100 μm.

Abbreviations and symbols: Ur: Urothelium; Lp: Lamina propria; white arrow, conjunctive-vascular axis; black arrow, basal membrane integrity; star, cell atypia; triangle, cellular cords; PDH: Pyruvate dehydrogenase; CS: Citrate synthase; HADHSC: Short chain 3-hydroxyacyl-CoA dehydrogenase; ATP: Adenosine triphosphate.

Similarly, significant increase in immunoreactivity was observed for GAPDH and LDH in both the high-grade pTa and pT1 groups, as indicated in Figure 5H, I, K and L, in comparison to the normal (Figure 2G and H) and low-grade pTa groups (Figure 5G and J), which recorded weak immunoreactivity for the same proteins (Table 2). Moreover, no statistically significant differences in immunoreactivity toward hsp60 (Figure 2I, 5M, 5N, and 5O) were observed among the groups, although all of them recorded intense immunoreactivity (Table 2).

There was significant increase in GLUT1, PFK, and GAPDH protein levels in both the high-grade pTa and pT1 groups in comparison to the normal and low-grade pTa groups, as shown in Figures 4E, 4F, and 6A. Interestingly, the pT1 group recorded the highest LDH protein levels in comparison to the other groups, as highlighted in Figure 6B. Furthermore, no statistically significant differences in LDH protein levels were found between low-grade pTa and high-grade pTa groups, which were significantly higher in relation to normal group (Figure 6B).

In addition, no statistically significant differences in hsp60 protein levels were found among the groups, as shown in Figure 6C.

3.4. IBEC was significantly lower in high-grade pTa and high-grade pT1 bladder tumors

An assessment involving the IBEC calculation was performed. Based on the results, normal bladder tissue

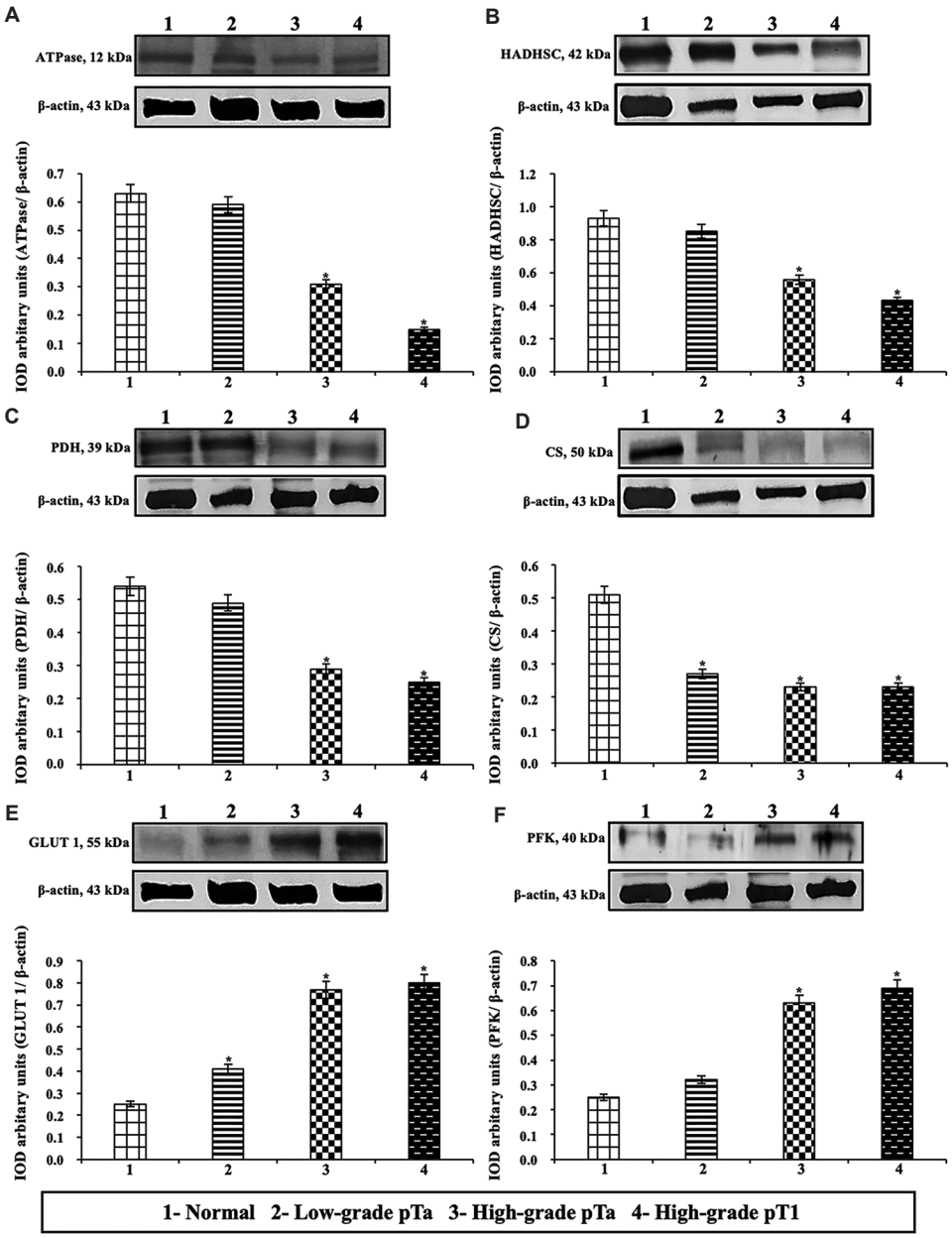


Figure 4. Representative immunoblotting analysis results and semi-quantitative determination of β-F1-ATP synthase (ATPase) (A), HADHSC (B), PDH (C), CS (D), GLUT 1 (E), and PFK (F) protein levels. Representative protein profiles pooled from ten patients per group for each repetition (duplicate). Graphs depict the relative expression of integrated optical density observed for β-F1-ATP synthase (ATPase), HADHSC, PDH, CS, GLUT 1, and PFK proteins, normalized by β-actin and expressed as mean ± standard deviation. *Significance difference ($P < 0.01$), after applying Tukey test.
Abbreviations: ATP: Adenosine triphosphate; GLUT1: Glucose transporter-1; PFK: Phosphofructokinase; PDH: Pyruvate dehydrogenase; CS: Citrate synthase; HADHSC: Short chain 3-hydroxyacyl-CoA dehydrogenase.

and low-grade pTa tumors recorded notably higher IBEC values than both high-grade pTa and pT1 tumors, as graphically represented in Figure 7.

4. Discussion

The primary treatment approach to NMIBC typically involves surgical intervention via TURBT. This procedure allows removing visible lesions and collecting tissue samples for histopathological analysis purposes, and it enables determining tumor stage and grade. Intravesical chemotherapy is often administered as adjunctive measure for NMIBC treatment within 6 h after TURBT to prevent tumor cells' post-procedure implantation and to reduce relapse rates.[24] Another adjuvant therapy option is BCG

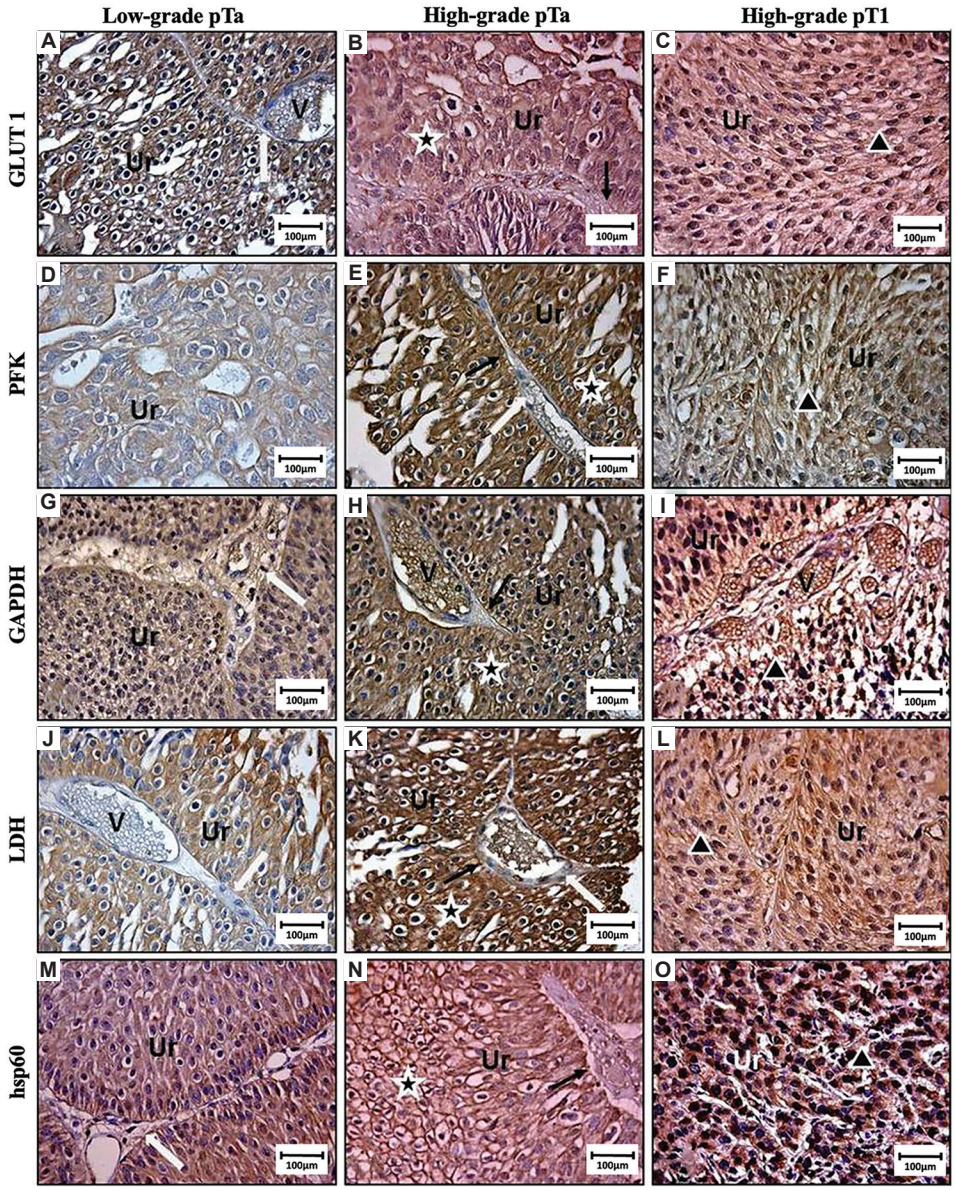


Figure 5. Immunohistochemical results of urinary bladder in low-grade pTa (A, D, G, J, and M), high-grade pTa (B, E, H, K, and N), and high-grade pT1 (C, F, I, L, and O) groups. Cytoplasmic immunoreactivity was observed for GLUT1 (A-C), PFK (D-F), GAPDH (G-I), LDH-A (J-L), and hsp60 (M-O) protein levels in urothelial cells.

Abbreviations and symbols: Ur: Urothelium; V: Blood vessel; white arrow, conjunctive-vascular axis; black arrow, basal membrane integrity; star, cell atypia; triangle, cellular cords; GLUT1: Glucose transporter-1; PFK: Phosphofructokinase; GAPDH: Glyceraldehyde 3-phosphate dehydrogenase; LDH-A: Lactate dehydrogenase A; hsp60: Heat shock protein 60.

immunotherapy, which is administered 4 to 6 weeks after TURBT application to allow resected area re-epithelialization and to minimize the risk of bacterial dissemination within the body.[6] Nowadays, BCG immunotherapy stands out as the preferred treatment to be applied to high-grade NMIBC cases, given its higher effectiveness in comparison to intravesical chemotherapy, mainly when it comes to tumor relapse and progression rates.[6,25]

However, using attenuated living organisms, such as BCG, can lead to side effects and pose challenges to predicting patient responses. Side effects occur in more than 90% of patients undergoing BCG treatment. They range from mild to moderate irritative urinary tract symptoms to severe complications, such as hemodynamic instability, persistent fever or allergic reactions that can compromise BCG usage.[25-27] Given these considerations, a

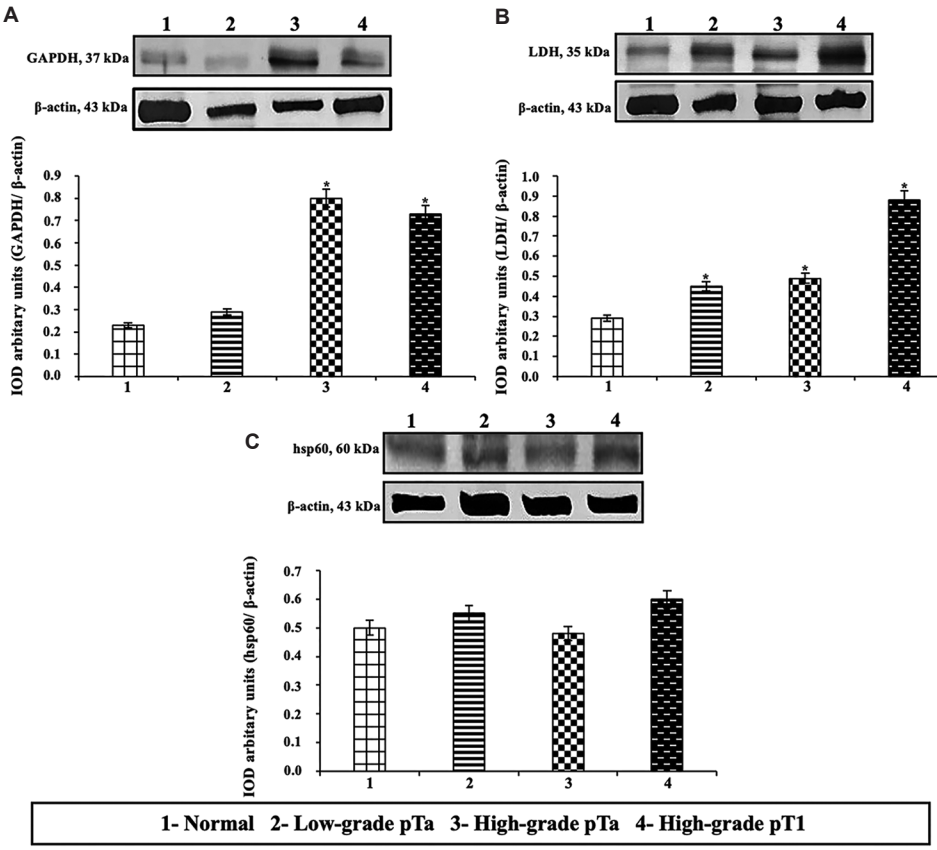


Figure 6. Representative immunoblotting analysis results and semi-quantitative determination of GAPDH (A), LDH (B), and hsp60 (C) protein levels. Representative protein profiles pooled from ten patients per group for each repetition (duplicate). Graphs depict the relative expression of integrated optical density observed for GAPDH, LDH, and hsp60 proteins, normalized by β-actin and expressed as mean ± standard deviation. *Significance difference ($P < 0.01$), after applying Tukey test.
Abbreviations: GAPDH: Glyceraldehyde 3-phosphate dehydrogenase; LDH: Lactate dehydrogenase; hsp60: Heat shock protein 60.

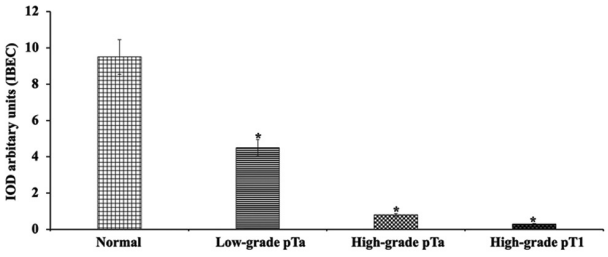


Figure 7. Bioenergetic cellular index observed for normal, low-grade pTa, high-grade pTa and high-grade pT1 groups. The presented results are expressed as mean ± standard deviation. Different lowercase letters (**A-C**) indicate significant differences ($P < 0.01$) between groups, after applying Tukey test. *Significance difference ($P < 0.01$), after applying Tukey test.

series of studies have been conducted to explore alternative therapies that can effectively eradicate NMIBC and introduce lesser detrimental effects on patients' body.

The aims of the present study were to feature and compare cell energy metabolism profiles among different histological NMIBC grades. Moreover, the IBEC was adjusted to these tumor types. Such an association between NMIBC and cell energy metabolism holds particular significance to establish clinical-pathological and prognostic criteria, as well as to further develop new, highly effective therapies targeting the metabolism of these tumor cells without causing much side effects.

Our results demonstrated notable difference in energy metabolism among normal bladder tissue, and low-grade (low-grade pTa group) and high-grade (high-grade pTa and pT1 groups) NMIBC. Normal bladder tissue and low-grade tumors showed preference for the oxidative phosphorylation pathway, whereas high-grade tumors leaned toward glycolytic metabolism. These findings were based on the analysis applied to several metabolic pathway-related proteins.

Normal bladder tissue and low-grade pTa tumors presented high IBEC due to their prevalent reliance on oxidative phosphorylation, which was evidenced by intense immunoreactivity and high β-F1-ATP synthase

Table 2. Mean immunolabelled antigen intensities in urinary bladder samples collected from normal, low-grade pTa, high-grade pTa, and high-grade pT1 groups

Antigens	Groups			
	Normal (*n*=10) (%)	Low-grade pTa (*n*=10) (%)	High-grade pTa (*n*=10) (%)	High-grade pT1 (*n*=10) (%)
β-F1-ATP synthase	3 (92.7)*	3 (86.2)*	2 (41.3)	1 (15.1)
HADHSC	3 (91.1)*	3 (90.5)*	2 (61.7)	1 (17.9)
PDH	3 (83.0)*	3 (85.9)*	2 (51.1)	1 (19.3)
CS	3 (88.4)*	3 (94.8)*	2 (52.5)	1 (23.0)
GLUT1	1 (17.3)	1 (29.7)	3 (89.9)*	3 (79.7)*
PFK	1 (24.9)	1 (32.0)	3 (94.2)*	3 (92.1)*
GAPDH	1 (19.8)	1 (29.3)	3 (85.2)*	3 (76.4)*
LDH	1 (30.2)	1 (27.4)	3 (94.7)*	3 (88.2)*
hsp60	3 (93.5)*	3 (89.2)*	3 (87.1)*	3 (81.9)*

Notes: 0, lack of immunoreactivity; 1, weak immunoreactivity (1 – 35% positive urothelial cells); 2, moderate immunoreactivity (36 – 70% positive urothelial cells); 3, intense immunoreactivity (>70% positive urothelial cells). *Statistical significance (proportion test, $P<0.0001$). Abbreviations: ATP: Adenosine triphosphate; GLUT1: Glucose transporter-1; PFK: Phosphofructokinase; GAPDH: Glyceraldehyde 3-phosphate dehydrogenase; LDH: Lactate dehydrogenase; PDH: Pyruvate dehydrogenase; CS: Citrate synthase; HADHSC: Short chain 3-hydroxyacyl-CoA dehydrogenase; hsp60: Heat shock protein 60.

protein levels, in association with weak immunoreactivity and reduced GAPDH protein levels. These tumors also presented intense immunoreactivity and high HADHSC and PDH protein levels, in addition to weak immunoreactivity and decreased GLUT1 and PFK protein levels.

Increased β-F1-ATP synthase activity indicates increased mitochondrial activity, since this protein crosses the mitochondrial inner membrane and accounts for ADP conversion into ATP. This process takes place through ADP combination to a free ionic phosphate radical, which adds another high energy phosphate bond to the molecule. The final process happens when ATP is transported by facilitated mitochondria diffusion into the cytoplasm. After the entire process, each glucose molecule generated 38 ATPs, carbon dioxide, and water.[13-16] The HADHSC protein transforms fatty acid into acetyl-coA, and PDH transforms pyruvate into acetyl-coA, and both of them transform different substrates into acetyl-coA in order to generate energy in the mitochondria. These proteins are closely related to oxidative phosphorylation, and this is the typical, normal mode of cell metabolism, since it does not deviate from the metabolic pathway to generate other substrates, as well as because it happens in an environment presenting normal oxygen levels.[13] Therefore, high IBEC in these tumors may point out good prognosis, besides helping therapeutic decision-making and these patients' follow-up.

The CS protein only recorded difference in immunoreactivity between low- and high-grade tumors, but it did not show changes in protein levels between these groups. Interestingly, CS protein levels were significantly higher in normal bladder tissue when compared to different NMIBC grades. It may have happened because this enzyme is directly linked to pathway speed, rather than to deviations in metabolic pathways. However, further studies focused on investigating the actual role played by this enzyme in NMIBC metabolism should be conducted.[28]

Immunohistochemistry and Western blotting results observed for high-grade pTa and high-grade pT1 tumors were quite consistent with each other, but they differed from those observed for normal bladder tissue and low-grade pTa tumors. The high-grade pTa and high-grade pT1 tumors manifested intense-to-moderate immunoreactivity for proteins associated with glycolytic pathway, as well as higher GLUT1, PFK, and GAPDH protein levels. They also presented weak immunoreactivity and low β-F1-ATP synthase, HADHSC, and PDH protein levels. Thus, they presented IBEC lower than that of normal bladder tissue and low-grade tumors.

Low IBEC in high-grade tumors highlights significant changes in the energy metabolism of normal cells. As previously suggested by Otto Warburg, the energy metabolic activity of malignant neoplasms is mostly concentrated in the glycolytic pathway.[13] Increased metabolism in tumor cells requires higher ATP consumption, and since the glycolytic pathway produces less ATP than oxidative phosphorylation, although much faster, some enzymes present increased activity to promptly meet the energy needs of these cells. GLUT1 belongs to the GLUT molecules' family and wields paramount importance in this scenario, since it accounts for allowing glucose to enter the cells. The literature reported increased activity of this protein in a series of neoplasms, such as pancreatic, ovarian and kidney cancer, among others.[29] This glucose avidity can be measured through positron emission tomography-computed tomography, an examination tool used to assess the metabolism of structures based on radiotracer glucose uptake determined by F18-fluorordesoxyglucose radiopharmaceutical. Lesions presenting high radiotracer glucose uptake are metabolically active. Consequently, they become more aggressive.[30] The major BC indications comprise lymph node staging, distant metastasis and relapse after definitive treatment.[30]

Cancer cells present increased glucose and glutamine uptake during cancer invasiveness progression, mostly by

increasing the expression of GLUT1 transporters on their surface.[11,12] This increased glucose uptake sets the stage for metabolic competition between effector T cells and tumor cells.[31] Notably, differentiated $CD8^+$ T cells present increased reliance on glucose-dependent metabolism in comparison to their naïve counterparts. Consequently, glucose shortage negatively impacts the effector functions of $CD8^+$ T cells, leading to compromised immune response and potentially limiting immune checkpoint therapy effectiveness.[31] Furthermore, proapoptotic Bcl-2 family members are activated and promote cell apoptosis when glucose uptake is limited.[11,32] Recent studies have suggested that limited glucose consumption in T cells can be mitigated through inosine or fatty acid metabolism modulation, although further investigations in this field should be conducted.[11,32,33]

As the active players in glycolysis, PFK and GAPDH play important role in glucose degradation and energy generation processes. LDH is another essential protein for tumor cell metabolism, since it enables pyruvate conversion into lactate, which is transported out of the cytoplasm to be used by the same cell to produce other molecules or to be used by the neighboring cells. This process ensures tumor cell energy production and substrate supply, even in hypoxic and acidic environment, due to high metabolism and low perfusion. This acidic environment protects the tumor cell from apoptosis and enables the invasion of other tissues.[34,35] LDH indices in the current study were higher in high-grade pT1 tumors than in the other types, likely because it is a more undifferentiated tumor. Thus, low IBEC in these neoplasms can be an unfavorable factor that can be used in therapeutic decision-making, mainly to indicate another TURBT (Re-TURBT) procedure or even early radical cystectomy.

There was no change in mitochondrion structure among the investigated groups, neither in immunoreactivity nor in hsp60 protein levels. This finding indicates that mitochondrial function can be restored in high-grade tumor cases showing decreased oxidative phosphorylation, as previously observed by Fantin *et al.*[36]

High-grade pTa tumors presented metabolic behavior quite similar to that of pT1 tumors, high relapse likelihood and progression to muscle-invasive disease; therefore, they must be subjected to aggressive treatment. High-grade pT1 tumors must be subjected to Re-TURBT, from 4 to 6 weeks after the first resection, mainly if there is proper muscle absence at the first resection, since this change in protocol is observed in 10 – 25% of cases.[37] Other prognostic factors that should be taken into consideration in therapeutic decision-making comprise multifocality (>3 lesions), tumors larger than 3 cm, previous treatment with BCG, and presence of associated CIS.[6,25,27] Based on a multi-institute retrospective study conducted with 2,451 high-grade pT1 patients who were analyzed after treatment with BCG, Re-TURBT was beneficial to progression-free survival, as well as to overall survival, although only in cases showing proper muscle absence after the first TURBT.[38] Results in the current study are unprecedented; thus, using IBEC in clinical practice presents a potential strategy for aiding therapeutic decision-making, mainly for high-grade pTa tumor cases, which are often not aggressively treated as pT1 tumors. Cuezva *et al.*[23] assessed IBEC in lung adenocarcinomas and observed that it was lower in large tumors (>3 cm) than in smaller tumors and than in lungs without neoplasm. IBEC was also correlated to tumor stage. IA-stage tumors recorded IBEC 2.5 times higher than IB-stage tumors, and it evidenced clear IBEC correlation to disease prognosis.

Some high-grade tumors can relapse and progress to muscle-invasive tumors during follow-up, even after aggressive local treatment application (TURBT + Re-TURBT + BCG). These patients have worse prognosis than those with muscle-invasive disease as the initial presentation. Moschini *et al.*[39] retrospectively investigated a group of 768 patients subjected to radical cystectomy due to muscle-invasive tumors (475 patients), or due to superficial tumors that had progressed to muscle-invasive stage, even after intravesical therapies, during follow-up (293 patients). They observed that the non-muscle-invasive group that had progressed during follow-up recorded worse results for progression/relapse-free survival, cancer-specific mortality, and overall mortality within 10 years, based on univariate and multivariate analyses.[39] Therefore, patients with pT1-grade NMIBC should be subjected to aggressive treatments, such as early radical cystectomy, mainly in case of BCG failure after TURBT and Re-TURBT. Since high-grade pTa tumors were metabolically similar to pT1, they should be treated in the same way as pT1, especially if they show low IBEC. Therefore, IBEC determination can be treated as an additional tool to help managing these cases, particularly under the concerns that treatments applied to them are quite aggressive and often lead to significant morbidity.

5. Conclusion

The aims of the current study were to both feature and compare cell energy metabolism profiles among normal bladder tissue and NMIBC tissues of different histological grades (such as low-grade pTa, high-grade pTa, and high-grade pT1 tumors). In addition, this study introduced the concept of IBEC, which is a new approach applicable to treat these tumors. In summary, according to the current

findings, normal bladder tissue, and low-grade pTa tumors mostly rely on oxidative phosphorylation as primary energy metabolism pathway, which contributes to high IBEC. On the other hand, high-grade pTa and high-grade pT1 tumors present prevalent glycolytic metabolism profile over oxidative phosphorylation, which leads to the lower IBEC.

In conclusion, the abnormal values of IBEC observed for NMIBC grades underscore its potential as a valuable marker in both the diagnosis and prognosis of BC patients.

Acknowledgments

The authors wish to express their gratitude for the assistance provided by the Amaral Carvalho Hospital (HAC), Jaú City, São Paulo State, Brazil, and the Program in Surgery Sciences of School of Medicine, Universidade Estadual de Campinas (UNICAMP), Campinas City, São Paulo State, Brazil.

Funding

This research was funded by the São Paulo Research Council (FAPESP grant numbers: 2014/11866-1; 2014/12047-4; 2018/10052-1; 2020/03419-6), and the Brazilian National Council for Scientific and Technological Development (CNPq grant numbers: 552120/2011-1; 312396/2021-0).

Conflict of interest

The authors declare that they have no competing interests.

Author contributions

Conceptualization: Guilherme Prado Costa, Petra Karla Böckelmann, Wagner José Fávaro

Formal analysis: Guilherme Prado Costa, Petra Karla Böckelmann, Leandro Luiz Lopes de Freitas, Gabriela Cardoso de Arruda Camargo, Gabriela de Oliveira, Bianca Ribeiro de Souza, Athanase Billis, Wagner José Fávaro

Investigation: Guilherme Prado Costa, Petra Karla Böckelmann, Renato Prado Costa, Carlos Hermann Schaal, Fernando César Sala, André Pereira Vanni, Leandro Luiz Lopes de Freitas, João Carlos Cardoso Alonso, Athanase Billis, Wagner José Fávaro

Methodology: Guilherme Prado Costa, Petra Karla Böckelmann, Leandro Luiz Lopes de Freitas, João Carlos Cardoso Alonso, Gabriela Cardoso de Arruda Camargo, Gabriela de Oliveira, Bianca Ribeiro de Souza, Athanase Billis, Wagner José Fávaro

Writing – original draft: Guilherme Prado Costa, Petra Karla Böckelmann, Wagner José Fávaro

Writing – review & editing: Guilherme Prado Costa, Wagner José Fávaro

Ethics approval and consent to participate

The study was conducted according to the guidelines of the Declaration of Helsinki and approved by the Institutional Ethics Committee of Ethics and Research Committee of Amaral Carvalho Hospital, Jaú City, São Paulo State, Brazil (CAAE number: 47475815.9.0000.5434). Informed consent was obtained from all subjects involved in the study.

Consent for publication

Written informed consent has been obtained from the patients to publish this paper.

Availability of data

The data presented in this study are available from the corresponding author on reasonable request.

References

1. Celada Luis G, Albers Acosta E, De la Fuente H, *et al*. A comprehensive analysis of immune response in patients with non-muscle-invasive bladder cancer. *Cancers* (*Basel*). 2023;15:1364.

   doi: 10.3390/cancers15051364

2. Bray F, Ferlay J, Soerjomataram I, Siegel RL, Torre LA, Jemal A. Global cancer statistics 2018: GLOBOCAN estimates of incidence and mortality worldwide for 36 cancers in 185 countries. *CA Cancer J Clin*. 2018;68:394-424.

   doi: 10.3322/caac.21492

3. Allard P, Bernard P, Fradet Y, Têtu B. The early clinical course of primary Ta and T1 bladder cancer: A proposed prognostic index. *Br J Urol*. 1998;81:692-698.

   doi: 10.1046/j.1464-410x.1998.00628.x

4. Lamm D, Persad R, Brausi M, *et al*. Defining progression in nonmuscle invasive bladder cancer: It is time for a new, standard definition. *J Urol*. 2014;191:20-27.

   doi: 10.1016/j.juro.2013.07.102

5. Babjuk M, Burger M, Capoun O, *et al*. European association of urology guidelines on non-muscle-invasive bladder cancer (Ta, T1, and carcinoma *in situ*). *Eur Urol*. 2022;81(1):75-94.

   doi: 10.1016/j.eururo.2021.08.010

6. Sylvester RJ, Van der Meijden AP, Oosterlinck W, *et al*. Predicting recurrence and progression in individual patients with stage Ta T1 bladder cancer using EORTC risk tables: A combined analysis of 2596 patients from seven EORTC trials. *Eur Urol*. 2006;49(3):466-465, discussion 475-477.

   doi: 10.1016/j.eururo.2005.12.031

7. Van Rhijn BW, Burger M, Lotan Y, *et al*. Recurrence and progression of disease in non-muscle-invasive bladder cancer: From epidemiology to treatment strategy. *Eur Urol*.

2009;56:430-442.

doi: 10.1016/j.eururo.2009.06.028

8. Cote RJ, Chatterjee SJ. Molecular determinants of outcome in bladder cancer. *Cancer J Sci Am.* 1999;5:2-15.

9. Humphrey PA, Moch H, Cubilla AL, Ulbright TM, Reuter VE. The 2016 WHO classification of tumours of the urinary system and male genital organs-part B: Prostate and bladder tumours. *Eur Urol.* 2016;70:106-119.

doi: 10.1016/j.eururo.2016.02.028

10. Kunju LP, You L, Zhang Y, Daignault S, Montie JE, Lee CT. Lymphovascular invasion of urothelial cancer in matched transurethral bladder tumor resection and radical cystectomy specimens. *J Urol.* 2008;180:1928-1932.

doi: 10.1016/j.juro.2008.07.056

11. Semeniuk-Wojtaś A, Poddębniak-Strama K, e, *et al*. Tumour microenvironment as a predictive factor for immunotherapy in non-muscle-invasive bladder cancer. *Cancer Immunol Immunother.* 2023;72(7):1971-1989.

doi: 10.1007/s00262-023-03376-9

12. Domblides C, Lartigue L, Faustin B. Control of the antitumor immune response by cancer metabolism. *Cells.* 2019;8(2):104.

doi: 10.3390/cells8020104

13. Hanahan D, Weinberg RA. Hallmarks of cancer: The next generation. *Cell.* 2011;144:646-674.

doi: 10.1016/j.cell.2011.02.013

14. DeBerardinis RJ, Lum JJ, Hatzivassiliou G, Thompson CB. The biology of cancer: Metabolic reprogramming fuels cell growth and proliferation. *Cell Metab.* 2008;7:11-20.

doi: 10.1016/j.cmet.2007.10.002

15. Vander Heiden MG, Cantley LC, Thompson CB. Understanding the Warburg effect: The metabolic requirements of cell proliferation. *Science.* 2009;324:1029-1033.

doi: 10.1126/science.1160809

16. Cairns RA, Harris IS, Mak TW. Regulation of cancer cell metabolism. *Nat Rev Cancer.* 2011;11:85-95.

doi: 10.1038/nrc2981

17. Cuezva JM, Krajewska M, De Heredia ML, *et al.* The bioenergetic signature of cancer: A marker of tumor progression. *Cancer Res.* 2002;62:6674-6681.

18. Isidoro A, Martínez M, Fernández PL, *et al*. Alteration of the bioenergetic phenotype of mitochondria is a hallmark of breast, gastric, lung and oesophageal cancer. *Biochem J.* 2004;378:17-20.

doi: 10.1042/BJ20031541

19. Vallejo CG, Cruz-Bermudez A, Clemente P, Hernandez-Sierra R, Garesse R, Quintanilla M. Evaluation of mitochondrial function and metabolic reprogramming during tumor progression in a cell model of skin carcinogenesis. *Biochimie.* 2013;95:1171-1176.

doi: 10.1016/j.biochi.2013.01.001

20. Epstein JI, Amin MB, Reuter VR, Mostofi FK. The world health organization/International society of urological pathology consensus classification of urothelial (transitional cell) neoplasms of the urinary bladder. Bladder Consensus Conference Committee. *Am J Surg Pathol.* 1998;22:1435-1448.

doi: 10.1097/00000478-199812000-00001

21. Fávaro WJ, Alonso JC, De Souza BR, *et al*. New synthetic nano-immunotherapy (OncoTherad®) for non-muscle invasive bladder cancer: Its synthesis, characterization and anticancer property. *Tissue Cell.* 2023;80:101988.

doi: 10.1016/j.tice.2022.101988

22. Reis IB, Tibo LH, Socca EA, De Souza BR, Durán N, Fávaro WJ. OncoTherad® (MRB-CFI-1) nano-immunotherapy reduced tumoral progression in non-muscle invasive bladder cancer through activation of Toll-like signaling pathway. *Tissue Cell.* 2022;76:101762.

doi: 10.1016/j.tice.2022.101762

23. Cuezva JM, Chen G, Alonso AM, *et al*. The bioenergetic signature of lung adenocarcinomas is a molecular marker of cancer diagnosis and prognosis. *Carcinogenesis.* 2004;25:1157-1163.

doi: 10.1093/carcin/bgh113

24. O'Donnell MA. Practical applications of intravesical chemotherapy and immunotherapy in high-risk patients with superficial bladder cancer. *Urol Clin North Am.* 2005;32:121-131.

doi: 10.1016/j.ucl.2005.01.003

25. Lobo N, Martini A, Kamat AM. Evolution of immunotherapy in the treatment of non-muscle-invasive bladder cancer. *Expert Rev Anticancer Ther.* 2022;22:361-370.

doi: 10.1080/14737140.2022.2046466

26. Böhle A, Brandau S. Immune mechanisms in bacillus Calmette-Guerin immunotherapy for superficial bladder cancer. *J Urol.* 2003;170:964-969.

doi: 10.1097/01.ju.0000073852.24341.4a

27. Wood D. Tumors of the bladder. In: Wein AJ, Kavoussi LR, Partin AW, Peters CA, editors. *Campbell-Walsh Urology*. 11th ed. Philadelphia, PA: Elsevier; 2016.

28. Lim HY, Ho QS, Low J, Choolani M, Wong KP. Respiratory competent mitochondria in human ovarian and peritoneal cancer. *Mitochondrion.* 2011;11:437-443.

doi: 10.1016/j.mito.2010.12.015

29. Macheda ML, Rogers S, Best JD. Molecular and cellular regulation of glucose transporter (GLUT) proteins in cancer.

J Cell Physiol. 2005;202:654-662.

doi: 10.1002/jcp.20166

30. Bouchelouche K, Choyke PL. PET/CT in renal, bladder and testicular cancer. *PET Clin.* 2015;10:361-374.

doi: 10.1016/j.cpet.2015.03.002

31. Renner K, Bruss C, Schnell A, *et al*. Restricting glycolysis preserves T cell effector functions and augments checkpoint therapy. *Cell Rep.* 2019;29:135-150.e9.

doi: 10.1016/j.celrep.2019.08.068

32. Wang T, Gnanaprakasam JN, Chen X, *et al*. Inosine is an alternative carbon source for CD8+-T-cell function under glucose restriction. *Nat Metab.* 2020;2:635-647.

doi: 10.1038/s42255-020-0219-4

33. Zhang Y, Kurupati R, Liu L, *et al*. Enhancing CD8+ T cell fatty acid catabolism within a metabolically challenging tumor microenvironment increases the efficacy of melanoma immunotherapy. *Cancer Cell.* 2017;32:377-391.e9.

doi: 10.1016/j.ccell.2017.08.004

34. Fischer K, Hoffmann P, Voelkl S, *et al*. Inhibitory effect of tumor cell-derived lactic acid on human T cells. *Blood.* 2007;109:3812-3819.

doi: 10.1182/blood-2006-07-035972

35. Swietach P, Vaughan-Jones RD, Harris AL. Regulation of tumor pH and the role of carbonic anhydrase 9. *Cancer Metastasis Rev.* 2007;26:299-310.

doi: 10.1007/s10555-007-9064-0

36. Fantin VR, St-Pierre J, Leder P. Attenuation of LDH-A expression uncovers a link between glycolysis, mitochondrial physiology, and tumor maintenance. *Cancer Cell.* 2006;9:425-434.

doi: 10.1016/j.ccr.2006.04.023

37. Kitamura H, Kakehi Y. Treatment and management of high-grade T1 bladder cancer: What should we do after second TUR? *Jpn J Clin Oncol.* 2015;45:315-322.

doi: 10.1093/jjco/hyu219

38. Gontero P, Sylvester R, Pisano F, *et al*. The impact of re-transurethral resection on clinical outcomes in a large multicentre cohort of patients with T1 high-grade/Grade 3 bladder cancer treated with bacille Calmette-Guerin. *BJU Int.* 2016;118:44-52.

doi: 10.1111/bju.13354

39. Moschini M, Sharma V, Dell'oglio P, *et al*. Comparing long-term outcomes of primary and progressive carcinoma invading bladder muscle after radical cystectomy. *BJU Int.* 2016;117:604-610.

doi: 10.1111/bju.13146